

## Critical behavior at the smectic-*A* to nematic transition confined to a random network

Sihai Qian, Germano S. Iannacchione, and Daniele Finotello

*Department of Physics and Liquid Crystal Institute, Kent State University, Kent, Ohio 44242*

(Received 27 November 1995)

The smectic-*A* to nematic (Sm-*A*-*N*) transition was studied confined to the randomly interconnected voids of Millipore filters via a high resolution calorimetry. The heat capacity peaks evolve from sharp and prominent to broad and small depending on void size. The random confinement drives the heat capacity critical exponent from the bulk value towards zero, indicating a confinement-induced decoupling of smectic and nematic order parameters. [S1063-651X(96)50605-7]

PACS number(s): 64.70.Md, 61.30.-v, 65.20.+w, 82.60.Fa

There continues to be a great deal of research in finite-size effects in the behavior of fluids imbedded in connected porous networks. The superfluid to normal transition of  $^4\text{He}$  [1] and the phase separation in binary liquid mixtures [2] are altered and new phenomena arise when they are confined to porous media of random geometry. Confined liquid crystal (LC) studies [3] are of growing interest as they possess several experimentally accessible phase transitions which allow to test the confinement influence on smectic formation, configurational transitions, orientational order, and effects on the critical behavior, studies that have attracted theoretical efforts [4]. The phase transitions, extensively studied in the bulk, involve different types of ordering, for instance orientational and translational. The bulk LC smectic-*A* to nematic (Sm-*A*-*N*) transition [5] is believed to belong to the three dimensional (3D) *XY* universality class ( $\alpha = -0.007$ ) and dominated by the strength of the coupling between the nematic orientational order parameter and the order parameter for the one-dimensional layered structure of the smectic-*A* (Sm-*A*) phase [6].

Two members of the alkylcyanobiphenyl *n*CB (*n* the number of carbons in the alkyl chain) LC series, 8CB and 9CB, exhibit the Sm-*A*-*N* transition. In bulk 8CB (nematic range  $\text{NR} \approx 7.1$  K), due to the coupling between smectic and nematic order parameters and director fluctuations, the Sm-*A*-*N* transition deviates from 3D *XY* universality to a non-universal crossover value between 3D *XY* and tricritical behavior with an effective heat capacity critical exponent  $\alpha$  ranging between 0.26 and 0.31 [5,7,8]. Because of the stronger coupling arising from its narrower NR ( $\approx 1.9$  K), the Sm-*A*-*N* transition for bulk 9CB is located at the tricritical point ( $\alpha = 0.5$ ) [9]. With increasing NR,  $\alpha$  decreases from the tricritical value  $\alpha = 0.5$  to  $\alpha \approx 0$  ( $\bar{n}$ S5 and *n*CB are two such cases [5]).

The 8CB Sm-*A*-*N* transition has been studied confined to Anopore [8], silica Aerogel [10–14], and Vycor glass [15]; the transition was either nonexistent or highly suppressed. Here, we report heat capacity measurements for 8CB and 9CB confined to the randomly interconnected voids of Millipore filters, as a function of void size. The Sm-*A*-*N* heat capacity peak is prominent and allows to determine the critical exponent  $\alpha$  as a function of confining size. Depending on void size and LC nematic range, the confinement strongly affects  $\alpha$  and the Sm-*A*-*N* transition enthalpy. Significant changes take place at an LC dependent “critical size.”

Millipore filters [16] are composed of pure biologically inert mixtures of cellulose acetate and cellulose nitrate. The manufacturer’s quoted (nominal) void sizes used were 0.025, 0.05, 0.1, 0.22, 0.8, and 5  $\mu\text{m}$ , which most likely represent the shortest length scale of the filters. From our scanning electron microscopy (SEM) studies, the actual average void size ranges from 0.2 to 7.5  $\mu\text{m}$ , with a wide void size distribution for each filter. ac calorimetry [17] was performed on samples made of a Millipore square ( $6 \times 6$  mm<sup>2</sup>,  $\sim 130$   $\mu\text{m}$  thick) filled with 2 to 4.5 mg of LC depending on the void size.

Heat capacity results for bulk 8CB and 9CB from the same LC batches used in the confinement studies, see Table I, are consistent with those in the literature [7–9]. In Fig. 1 we plot the excess Sm-*A*-*N* specific heat  $\Delta C_p$  for bulk and six confined 8CB samples, after subtraction of the low temperature wing of their respective nematic-isotropic (*N*-*I*) transition. The confined  $T_{\text{Sm-}A\text{-}N}$  (Table I), are shifted down from bulk, yet, no regular trend versus void size (or porosity) exists. Elastic constraints rather than finite-size effects dominate the observed behavior [13,14]. Interestingly, there is no significant change in the NR for either LC under all Millipore confinements.

At first, the transition peaks are sharp, but, with decreasing void size, they become broad, round and small. The divergent nature is lost starting with the 0.1  $\mu\text{m}$  sample. This is quantified by the FWHM (full width at half maximum) of the specific heat peak which increases from bulk to the 0.025  $\mu\text{m}$  sample, as listed in Table I. Normalizing by the bulk value [the ratio of FWHM to FWHM(bulk)] with decreasing void size the ratios are 1, 2.3, 2.7, 5.2, 11.3, 11.7, 17.8. A drastic increase takes place between the 0.22 and 0.1  $\mu\text{m}$  samples.

The effects of the Millipore confinement is also reflected in the Sm-*A*-*N* transition enthalpy, calculated from  $\Delta H_{\text{Sm-}A\text{-}N} = \int \Delta C_p dT$  over a  $T_{\text{Sm-}A\text{-}N} \pm 3$  K range; listed in Table I,  $\Delta H_{\text{Sm-}A\text{-}N}$  decreases with void size. As seen in Fig. 2, in Millipore, the pretransitional region is suppressed with respect to bulk, i.e.,  $\Delta C_p$  approaches zero at a temperature closer to its  $T_{\text{Sm-}A\text{-}N}$  than bulk. The enthalpy decrease is not consistent with a reduction of the bulk peak due to the suppression of smectic-*A* long range order as the correlation length saturates [13,14]. This is stressed in the inset to Fig. 2 where we plot the enthalpy difference from bulk, scaled by the bulk value [18] for Millipore, Aerogel [13], and finite-

TABLE I. Sm-A-N transition parameters for bulk and Millipore confined 8CB and 9CB.

	8CB			9CB		
	$T_{\text{Sm-A-N}}$ (K)	$\Delta H_{\text{Sm-A-N}}$ (J/g)	FWHM (mK)	$T_{\text{Sm-A-N}}$ (K)	$\Delta H_{\text{Sm-A-N}}$ (J/g)	FWHM (mK)
Bulk	306.95	$0.94 \pm 0.05$	$44 \pm 10$	321.21	$1.26 \pm 0.09$	$38 \pm 5$
5 $\mu\text{m}$	306.84	$0.69 \pm 0.05$	$103 \pm 13$			
0.8 $\mu\text{m}$	306.85	$0.65 \pm 0.05$	$119 \pm 13$	320.76	$1.1 \pm 0.05$	$50 \pm 6$
0.22 $\mu\text{m}$	306.83	$0.62 \pm 0.05$	$227 \pm 23$	320.53	$1.15 \pm 0.05$	$69 \pm 6$
0.1 $\mu\text{m}$	306.69	$0.56 \pm 0.05$	$497 \pm 37$			
0.05 $\mu\text{m}$	306.71	$0.44 \pm 0.05$	$516 \pm 31$	320.98	$1.2 \pm 0.05$	$71 \pm 7$
0.025 $\mu\text{m}$	306.18	$0.34 \pm 0.05$	$781 \pm 86$	320.81	$0.88 \pm 0.05$	$231 \pm 10$

size-limited correlation length. Under confinement, and more so in Millipore, the enthalpy is substantially suppressed as compared to finite size effects expectations.

The 9CB studies shown in Fig. 3 were performed on bulk and four Millipore sizes: 0.8, 0.22, 0.05, and 0.025  $\mu\text{m}$ . The heat capacity peaks retain a divergent nature except for the smallest void size. The FWHM increases with decreasing void size and the ratios with the respect to bulk are as follows: 1, 1.3, 1.8, 1.9, and 6.1, a slower increase rate than in 8CB with a similar drastic increase but now between the 0.05 and 0.025  $\mu\text{m}$  samples. The transition enthalpy also exhibits a weaker void size dependence. Determined over a narrower temperature range  $T_{\text{Sm-A-N}} \pm 1.1$  K due to 9CB's narrower NR,  $\Delta H_{\text{Sm-A-N}}$  is nearly constant with an average value of  $1.18 \pm 0.12$  J/g for bulk and confined to the three largest

samples. For the 0.025  $\mu\text{m}$  sample there is a 30% decrease from the bulk value.

Combining these results with deuterium NMR studies in confined systems that prove the existence of an orientationally ordered layer to temperatures deep in the isotropic phase [3], the decrease of enthalpy with decreasing void size can be understood in terms of a pinning model [8]. In smaller void sizes, a larger fraction of LC molecules are in direct contact with the confining substrate. The pinned material does not participate in the Sm-A-N transition at the same temperature as molecules farther away from the surface; the transition is consequently broad and suppressed as compared to bulk. Under extreme confinement, most molecules are pinned at the surfaces and the transition is replaced by a continuous evolution of local order as for  $n\text{CB}$  in Vycor glass [3,15].

The critical behavior is determined by fitting the excess specific heat data of Figs. 1 and 3 to a power law in reduced temperature including a correction-to-scaling term [5,19]:

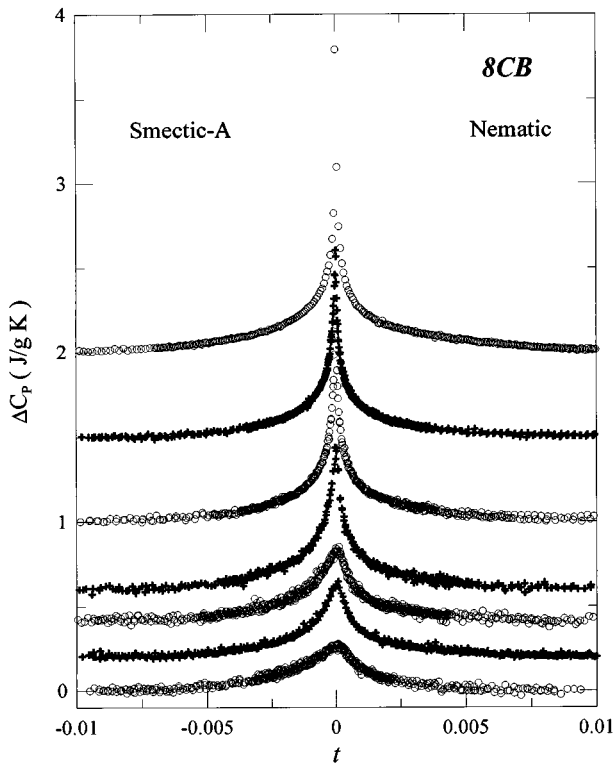


FIG. 1. Excess Sm-A-N specific heat of bulk and Millipore confined 8CB against reduced temperature. Data for bulk, 5, 0.8, 0.22, 0.10, and 0.05  $\mu\text{m}$  samples (upper to lower curves) are shifted up by 1.5, 1.0, 0.6, 0.4, and 0.2 J/g K, respectively. The 0.025  $\mu\text{m}$  data (lowest curve) are unshifted.

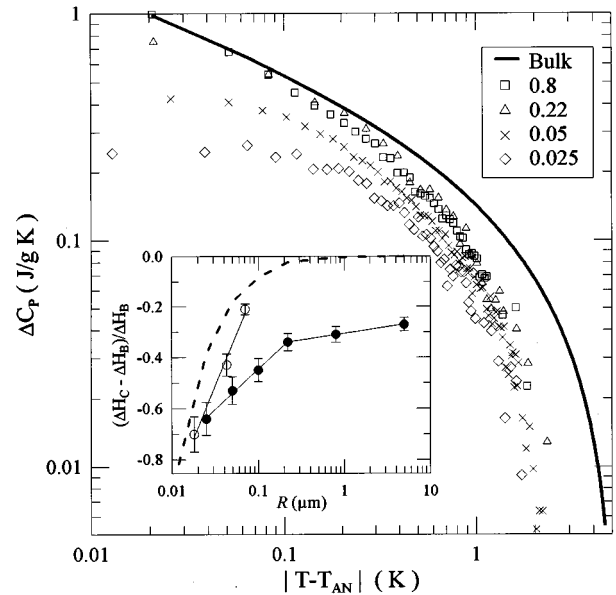


FIG. 2. Excess specific heat of bulk and Millipore confined 8CB vs temperature  $T_{\text{Sm-A-N}} - T$ . For clarity, only the  $T < T_{\text{Sm-A-N}}$  side of four of the samples are shown. Inset: enthalpy change of confined samples ( $\Delta H_C$ ) with respect to bulk ( $\Delta H_B$ ) vs void size. Millipore ( $\bullet$ ) and Aerogel ( $\circ$ ) results from [10] are included. Dashed line is the expected enthalpy due to a pure finite-size effect that truncates the heat capacity peak when the correlation length equals the nominal void size.

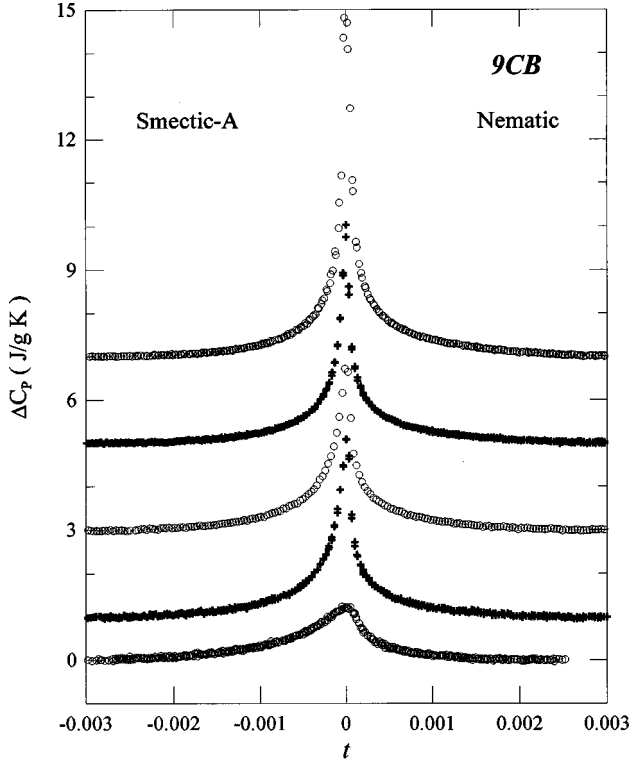


FIG. 3. Excess Sm-A-N specific heat of bulk and Millipore confined 9CB against reduced temperature. Data for bulk, 0.8, 0.22, and 0.05  $\mu\text{m}$  samples (upper to lower curves) are shifted up by 7, 5, 3, and 1 J/g K, respectively. The 0.025  $\mu\text{m}$  data (lowest curve) are unshifted.

$$\Delta C_p = B_C + Lt + \frac{A_{\pm}}{\alpha} |t|^{-\alpha} (1 + D_{\pm} |t|^{1/2}),$$

$$t = (T - T_{\text{Sm-A-N}}) / T_{\text{Sm-A-N}}, \quad (1)$$

The  $\pm$  subscripts indicate parameters above and below the transition temperature. The constant and linear terms are introduced to account for any remnant background. The factor  $A_{\pm}/\alpha$ , rather than  $A_{\pm}$ , allows  $\alpha$  to continuously vary about zero. Typically 300 data points at either side of  $T_{\text{Sm-A-N}}$  are simultaneously fitted using a method that includes standard range shrinking procedures after data points near the rounded central part are removed. The stability of the fits was evaluated as the reduced temperature shrunk from  $1.6 \times 10^{-2}$  to  $1 \times 10^{-3}$  for 8CB and  $8.5 \times 10^{-3}$  to  $4 \times 10^{-4}$  for 9CB.

For bulk 8CB,  $\alpha = 0.28 \pm 0.02$ , with an amplitude ratio  $A_-/A_+ = 1.09 \pm 0.05$ , in good agreement with literature values [5]. In Millipore, due to the suppressed pretransitional behavior, i.e., the different curvature compared to bulk, a smaller exponent is expected. As summarized in Table II, the exponent tends towards zero with decreasing void size. For the 5 and 0.8  $\mu\text{m}$  samples,  $\alpha$  decreases to 0.18, although a 35% reduction from bulk, still representing an effective exponent. With increased confinement,  $\alpha$  goes to  $\sim 0.025$ . Thus,  $\alpha$  tends to zero between 0.22 and 0.1  $\mu\text{m}$  which is concomitant with the changes in the FWHM and enthalpy, suggestive of a ‘‘critical’’ void size  $\sim 0.2 \mu\text{m}$  for 8CB. The behavior of  $\alpha$  and  $A_-/A_+$  is listed in Table II and plotted in Fig. 4.

TABLE II. Results of fits to Eq. (1) for bulk and Millipore confined 8CB and 9CB. The errors quoted are the statistical uncertainties.

	8CB		9CB	
	$\alpha$	$A_-/A_+$	$\alpha$	$A_-/A_+$
Bulk	$0.28 \pm 0.015$	$1.09 \pm 0.05$	$0.52 \pm 0.02$	$1.32 \pm 0.05$
5 $\mu\text{m}$	$0.17 \pm 0.01$	$1.07 \pm 0.05$		
0.8 $\mu\text{m}$	$0.18 \pm 0.01$	$1.1 \pm 0.05$	$0.51 \pm 0.01$	$1.56 \pm 0.05$
0.22 $\mu\text{m}$	$0.077 \pm 0.004$	$1.06 \pm 0.05$	$0.37 \pm 0.02$	$1.65 \pm 0.05$
0.1 $\mu\text{m}$	$0.029 \pm 0.002$	$1.04 \pm 0.05$		
0.05 $\mu\text{m}$	$0.020 \pm 0.001$	$1.02 \pm 0.05$	$0.36 \pm 0.02$	$1.53 \pm 0.05$
0.025 $\mu\text{m}$	$0.036 \pm 0.004$	$1.05 \pm 0.05$	$0.037 \pm 0.002$	$1.09 \pm 0.05$

As expected [9], a very close to the tricritical value of the heat capacity exponent,  $\alpha = 0.52$ , is obtained here for bulk 9CB, with  $A_-/A_+ = 1.32 \pm 0.05$ . For the 0.8  $\mu\text{m}$  sample,  $\alpha$  remains at the tricritical value. With a decrease to 0.22  $\mu\text{m}$ ,  $\alpha = 0.37$ , a nonuniversal crossover value. A near zero value,  $\alpha = 0.037$ , is obtained for the 0.025  $\mu\text{m}$  sample. No regular behavior for  $A_-/A_+$  is found in going from bulk to the confined samples. Combined with the earlier enthalpy and FWHM analysis, 0.025  $\mu\text{m}$  behaves as a ‘‘critical’’ void size for 9CB: most of the determined properties are quite distinct from those in the larger void sizes, as summarized in Table II.

The bulk Sm-A-N transition is either nonuniversal (8CB) or tricritical (9CB) due to their narrow NR. In Millipore, an intermediate (nonuniversal) exponent is obtained with  $R = 5, 0.8,$  and  $0.22 \mu\text{m}$  for 8CB and  $R = 0.22$  and  $0.05 \mu\text{m}$  for 9CB. Since, for a narrow nematic range, the coupling of order parameters and director fluctuation drive the Sm-A-N transition away from 3D XY universality [6], the randomly

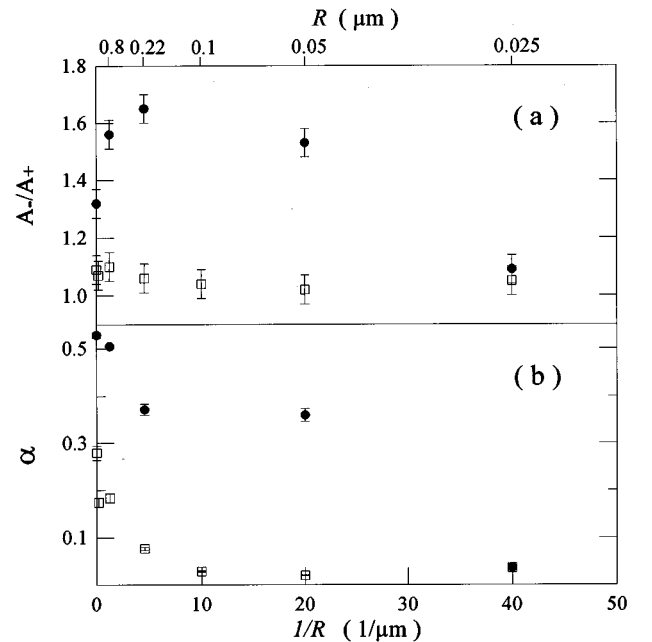


FIG. 4. Amplitude ratio (a) and specific heat exponent (b) for 8CB ( $\square$ ) and 9CB ( $\bullet$ ) against the inverse void size. Bulk results ( $1/R = 0 \mu\text{m}^{-1}$ ) are also included. Top x axis shows the void size.

interconnected voids of Millipore must have suppressed these fluctuations. This suggests a “truncation model” mechanism. The fluctuations are truncated to correlation lengths (wavelengths)  $\leq R$ . Further, since a bound (pinned) surface layer of LC exists, the strength of these fluctuations decreases for wavelengths approaching  $R$ . Long wavelength fluctuations, such as director fluctuations and the spatial fluctuations of the smectic layers are severely suppressed, while shorter wavelengths such as order parameter fluctuations, are restricted to a much lesser extent. This should be reflected in longer relaxation times for correlations as observed in quasi-elastic light scattering studies of 8CB in Aerogel [11]. Below a “critical” dimension,  $R_C$ , the smectic order parameter is effectively decoupled from the nematic one. The  $R_C$  ratio of 8CB to 9CB ( $\approx 0.2/0.05=4$ ) is tantalizingly close to the ratio of their nematic ranges ( $7.1/1.9=3.7$ ).

Other studies support this interpretation. If the order parameters coupling is increased (the NR decreased), one would expect to recover the bulk behavior. In  $0.05 \mu\text{m}$  Millipore, with the addition of 11% of non-nematic 10CB to 9CB, the NR is reduced by 30% and  $\alpha$  increases from 0.36 to

the tricritical value [20]. NMR studies for 8CB in several confining substrates show that the orientational order increases smoothly and unaffected by the Sm-A–N transition. This is contrast to bulk where a distinct increase in orientational order occurs at  $T_{\text{Sm-A-N}}$  [15,21].

In summary, the Millipore confinement alters the critical behavior and the enthalpy at the Sm-A–N transition. Reducing the void size has the same effect of an increase in NR in a bulk homologous series: it weakens the coupling between smectic and nematic order parameters. The transition enthalpy is suppressed in a manner not consistent with finite size effects; it agrees with expectations from the decoupling mechanism. The exponent  $\alpha$  is driven towards zero at a critical size which is smaller for a narrower NR LC material. Very likely,  $\alpha$  is approaching the 3D XY value of  $-0.007$ .

We acknowledge illuminating discussions with Noel Clark, Carl Garland, and David Johnson. This research was supported by the NSF-STC ALCOM Grant No. DMR 89-20147.

- 
- [1] M. H. W. Chan *et al.*, Phys. Rev. Lett. **61**, 1950 (1988); D. Finotello *et al.*, *ibid.* **61**, 1954 (1988); N. Mulders *et al.*, *ibid.* **67**, 695 (1991); N. Mulders and M. H. W. Chan, *ibid.* **75**, 3705 (1995); P. A. Crowell *et al.*, Phys. Rev. B **51**, 12 721 (1995).
- [2] P. Wiltzius *et al.*, Phys. Rev. Lett. **62**, 804 (1989); B. Frisken *et al.*, *ibid.* **66**, 2754 (1991); W. I. Goldburg *et al.*, Physica A **213**, 61 (1995).
- [3] G. Crawford *et al.*, Phys. Rev. Lett. **66**, 723 (1991); G. Iannacchione and D. Finotello, *ibid.* **69**, 2094 (1992); G. Iannacchione *et al.*, *ibid.* **71**, 2595 (1993); S. Tripathi *et al.*, *ibid.* **72**, 2725 (1994); S. Kralj *et al.*, Phys. Rev. E **48**, 340 (1993); A. Zidansek *et al.*, *ibid.* **51**, 3332 (1995).
- [4] A. Maritan *et al.*, Phys. Rev. Lett. **72**, 4113 (1994); K. Uzelac *et al.*, *ibid.* **74**, 422 (1995); A. Falicov and A. N. Berker, *ibid.* **74**, 426 (1995); Z. Zhang and A. Chakrabarti, Phys. Rev. E **52**, 4991 (1995).
- [5] C. W. Garland and G. Nounesis, Phys. Rev. E **49**, 2964 (1994).
- [6] B. I. Halperin, T. C. Lubensky, and S. K. Ma, Phys. Rev. Lett. **32**, 292 (1974); C. Dasgupta and B. I. Halperin, *ibid.* **47**, 1556 (1981); T. C. Lubensky, J. Chem. Phys. **80**, 31 (1981); B. R. Patton and B. S. Andereck, Phys. Rev. Lett. **69**, 1556 (1992).
- [7] G. B. Kastings *et al.*, J. Phys. (Paris) **41**, 879 (1980); J. Theon *et al.*, Phys. Rev. A **26**, 2886 (1982).
- [8] G. S. Iannacchione and D. Finotello, Phys. Rev. E **50**, 4780 (1994).
- [9] J. Theon *et al.*, Phys. Rev. Lett. **52**, 204 (1984).
- [10] T. Bellini *et al.*, Phys. Rev. Lett. **69**, 788 (1992).
- [11] T. Bellini *et al.*, Phys. Rev. Lett. **74**, 2740 (1995); X-l. Wu *et al.*, *ibid.* **69**, 470 (1992).
- [12] N. A. Clark *et al.*, Phys. Rev. Lett. **71**, 3505 (1993).
- [13] L. Wu *et al.*, Phys. Rev. E **51**, 2157 (1995).
- [14] A. G. Rappaport, N. A. Clark, B. N. Thomas, and T. Bellini, *Liquid Crystals in Complex Geometries Formed by Polymer and Porous Networks*, edited by G. P. Crawford and S. Zumer (Taylor & Francis, London, 1996).
- [15] G. Iannacchione *et al.*, Phys. Rev. E **53**, 2402 (1996).
- [16] Millipore Corp., 397 Williams St., Marlborough, MA 01752.
- [17] P. F. Sullivan and G. Seidel, Phys. Rev. **173**, 679 (1968).
- [18] There may be enthalpy variations among bulk LCs from different batches (see [10]).
- [19] A. Aharony and M. E. Fisher, Phys. Rev. B **37**, 4394 (1983), and references therein.
- [20] S. Qian, G. S. Iannacchione, and D. Finotello (unpublished).
- [21] G. S. Iannacchione *et al.* (unpublished).